SF2A 2016
L. Cambrésy, M. Deleuil, E. Pécontal, C. Reylé, J. Richard, L. Tresse and I. Vauglin (eds)

arXiv:1610.05031v1 [astro-ph.GA] 17 Oct 2016

UNDERSTANDING ACTIVE GALACTIC NUCLEI USING NEAR-INFRARED HIGH ANGULAR RESOLUTION POLARIMETRY II: PRELIMINARY RESULTS

F. Marin[1], L. Grosset[2], R. Goosmann[1], D. Gratadour[2], D. Rouan[2], Y. Clénet[2], D. Pelat[3] and P. Andrea Rojas Lobos[1]

Abstract. In this second research note of a series of two, we present the first near-infrared results we obtained when modeling Active Galactic Nuclei (AGN). Our first proceedings showed the comparison between the MontAGN and STOKES Monte Carlo codes. Now we use our radiative transfer codes to simulate the polarization maps of a prototypical, NGC 1068-like, type-2 radio-quiet AGN. We produced high angular resolution infrared (1 μm) polarization images to be compared with recent observations in this wavelength range. Our preliminary results already show a good agreement between the models and observations but cannot account for the peculiar linear polarization angle of the torus such as observed. Gratadour et al. (2015) found a polarization position angle being perpendicular to the bipolar outflows axis. Further work is needed to improve the models by adding physical phenomena such as dichroism and clumpiness.

Keywords: galaxies: active, galaxies: Seyfert, radiative transfer, techniques: polarimetric, techniques: high angular resolution

1 Introduction

Understanding the morphology, composition and history of each AGN component is a non-trivial goal that requires a strong synergy between all observational techniques. The role of polarimetric observations was highlighted in the 80s thanks to the discovery of broad Balmer lines and Fe II emission sharing a very similar polarization degree and position angle with the continuum polarization in NGC 1068, a type-2 AGN (Antonucci & Miller 1985). The resemblance of the polarized flux spectrum with respect to the flux spectrum of typical Seyfert-1s lead to the idea that Seyfert galaxies are all the same, at zeroth-order magnitude (Antonucci 1993). Observational difference would arise from a different orientation of the nuclei between pole-on and edge-on objects; this is due to the presence of an obscuring dusty region situated along the equatorial plane of the AGN that will block the direct radiation from the central engine for observers looking through the optically thick circumnuclear material. This is the concept of the so-called "dusty torus", first conceived by Rowan-Robinson (1977) and later confirmed by (Antonucci & Miller 1985).

Since then, a direct confirmation for the presence and structure of this dusty torus was an important objective for the AGN community. The closest evidence for a dusty torus around the central core of NGC 1068 was first obtained by Jaffe et al. (2004) and Wittkowski et al. (2004), using mid-infrared (MIR) and near-infrared (NIR) interferometric instruments coupled to the European Southern Observatory's (ESO's) Very Large Telescope interferometer (VLTI). Jaffe et al. (2004) were able to spatially resolve the MIR emission from the dusty structure and revealed that 320 K dust grains are confined in a 2.1 $\times$ 3.4 pc region, surrounding a smaller hot structure. The NIR data obtained by Wittkowski et al. (2004) confirm the presence of this region, with the NIR fluxes arising from scales smaller than 0.4 pc. Since then, long-baseline interferometry became a tool used to explore the innermost AGN dusty structure extensively at high angular resolution (typically of the order of milli-arcsec, see e.g., Kishimoto et al. 2009, 2011).

[1] Observatoire Astronomique de Strasbourg, Université de Strasbourg, CNRS, UMR 7550, 11 rue de l'Université, 67000 Strasbourg, France

[2] LESIA, Observatoire de Paris, PSL Research University, CNRS, Sorbonne Universités, UPMC Univ. Paris 06, Univ. Paris Diderot, Sorbonne Paris Cité

[3] LUTH, Observatoire de Paris, CNRS, Universit Paris Diderot, 92190 Meudon, France

© Société Francaise d'Astronomie et d'Astrophysique (SF2A) 2016

Coupling adaptive-optics-assisted polarimetry and high angular resolution observations in the infrared band, Gratadour et al. (2015) exploited the best of the two aforementioned techniques to obtain strong evidence for an extended nuclear torus at the center of NGC 1068. Similarly to previous optical (Capetti et al. 1995) and infrared (Packham et al. 1997; Lumsden et al. 1997) polarimetric observations, Gratadour et al. (2015) revealed an hourglass-shaped biconical structure whose polarization vectors point towards the hidden nucleus. By subtracting a purely centro-symmetric component from the map of polarization angles, an elongated (20×50 pc) region appeared at the assumed location of the dusty torus. If the signal traces the exact torus extension, high angular resolution polarization observations would become a very powerful tool to study the inner core of AGN.

In this lecture note, the second of the series, we will show the preliminary results obtained by running Monte Carlo radiative transfer codes for a NGC 1068-like AGN. Our ultimate goal is to reproduce the existing UV-to-infrared polarimetric observations using a single coherent model in order to constrain the true three-dimensional morphology of the hard-to-resolve components of close-by AGN.

2 Building an NGC 1068 prototype

Our primary model is powered by a central, isotropic, point-like source emitting an unpolarized spectrum with a power-law spectral energy distribution $F_* \propto \nu^{-\alpha}$ and $\alpha = 1$. Along the polar direction, a bi-conical, ionized wind with a 25° half-opening angle* with respect to the polar axis flows from the central source to 25 pc. The wind is assumed to be ionized and therefore filled with electrons. It is optically thin (optical depth in the V-band along polar direction $\tau_V = 0.1$). Along the equatorial plane, a flared disk sets on at 0.05 pc (a typical dust sublimation radius, see Kishimoto et al. 2007) and ends at 10 pc. The half-opening angle of the dust structure is fixed to 30° (Marin et al. 2012) and its V-band optical depth is of the order of 50. The dust is composed of 100 % silicates with grain radii ranging from 0.005 μm to 0.25 μm, together with a size distribution proportional to $a^{-3.5}$ (a being the grain radius).

The observer's viewing angle is set to 90° with respect to the symmetry axis of the model. More than 10^7 photons were sampled to obtain polarimetric images with a pixel resolution of 1 pc (9 milli-arcsec at 14.4 Mpc). For this proceedings note, we selected the images computed at 1 μm and used the Monte Carlo code STOKES.

2.1 Results of our baseline model

The polarimetric maps for our baseline model are shown in Fig. 1. The left image shows the polarization position angle superimposed to the 1 μm polarized flux. The polarization vectors show the orientation of polarization but are not proportional to the polarization degree (which is shown in the right image).

The polar outflows, where electron scattering occurs at a perpendicular angle, shows the strongest polarization degree (up to 90 – 100 %) associated with a centro-symmetric polarization angle pattern. This in perfect agreement with the polarization maps taken by the optical and infrared polarimeters in the 90s and recently upgraded by Gratadour et al. (2015). At the center of the model, the photon flux is heavily suppressed by the optically thick material, but scattered radiation from the cones to the surface of the torus leads to a marginal flux associated with a weak polarization degree† (< 8 %). Such degree of polarization is in very good agreement with the values observed by Gratadour et al. (2015) at the location of the nucleus (5 – 7 %). However, compared to the results of the previous authors, the polarization position angle from the modeling is almost centro-symmetric rather than aligned/anti-aligned with the circumnuclear dusty structure. It is only on the highest point of the torus morphology that a ~ 50 % polarization degree associated with a higher flux can be found, due to a lesser amount of dust facing the wind-scattered photon trajectories. When the whole picture is integrated, the resulting polarization degree is of the order of 60 %.

2.2 Accounting for the ISM

To test multiple configurations, we ran a second series.Based on the previous setup, we included interstellar matter (ISM) around the model. The ISM dust grains share the same composition as the dust in the circum-

*The half-opening angle of our model is smaller than what is observed (Goosmann & Matt 2011). We will change this value when the comparison between MontAGN and STOKES will be completed, see Paper I.

†Polarization degrees quoted in the text are for the scattered-induced polarization only. Dilution by the interstellar polarization, host galaxy starlight and starburst light will drastically reduce the observed polarization degree.

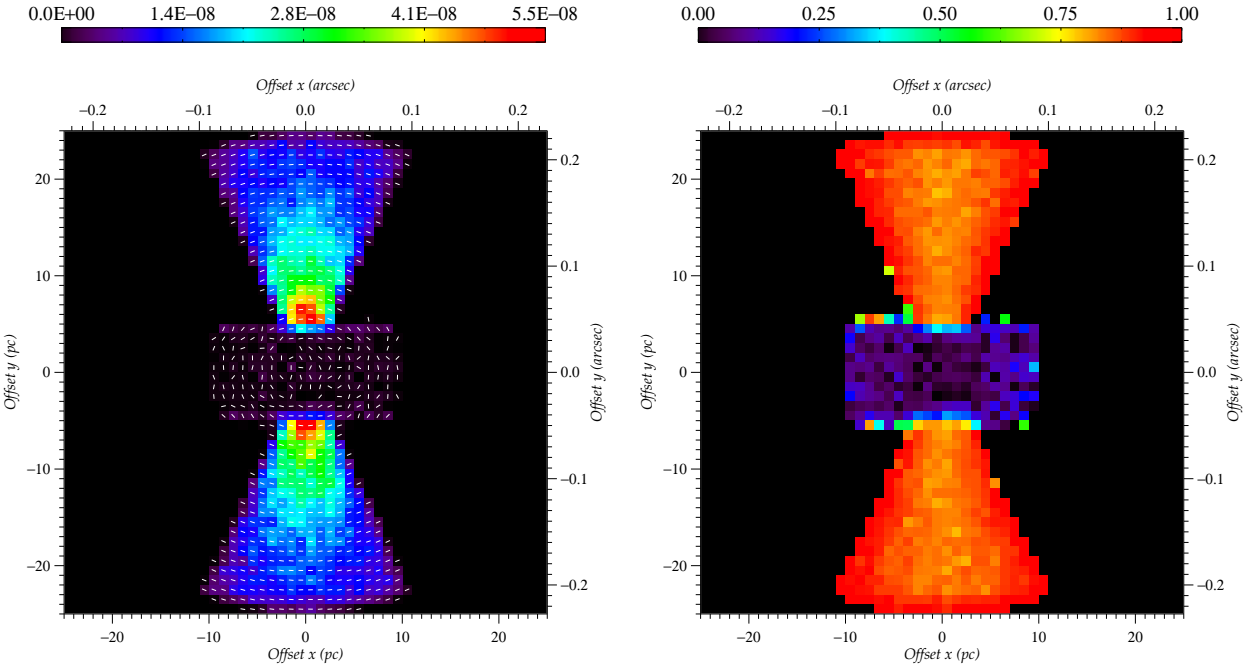

Fig. 1. 1 μm polarimetric simulations of NGC 1068. Left figure shows the color-coded polarized flux in arbitrary units with the polarization position angle superimposed to the image. Right figure shows the color-coded degree of polarization (from 0, unpolarized, to 1, fully polarized).

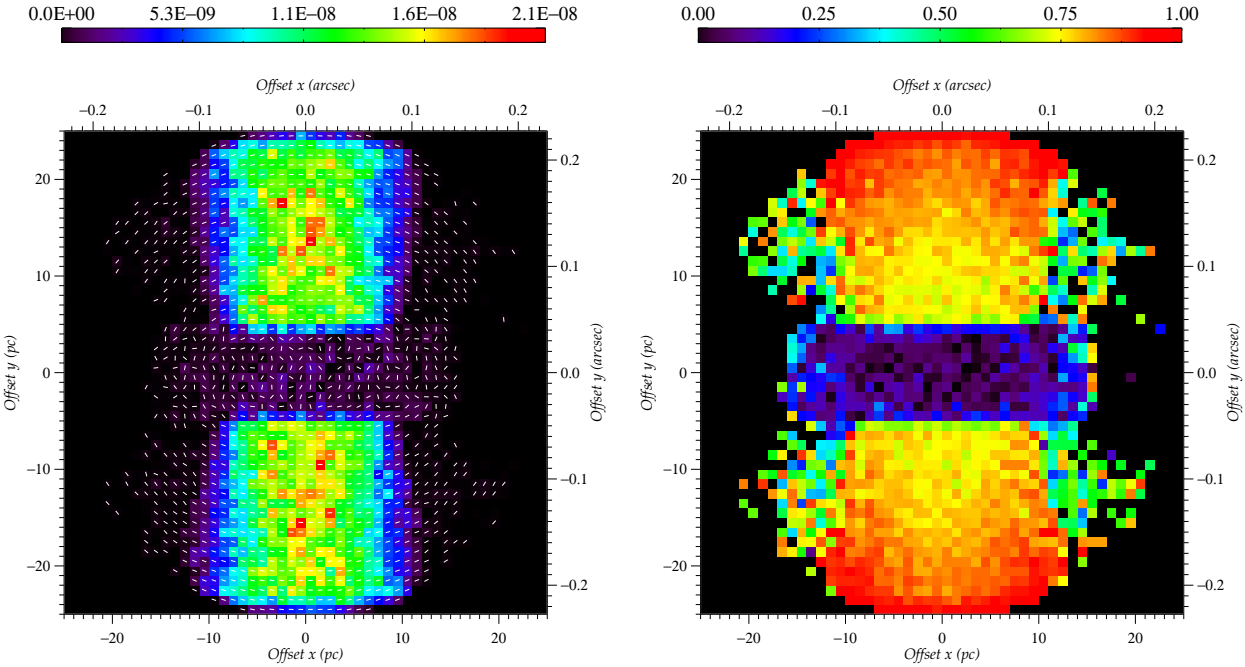

Fig. 2. Same as Fig. 1 with the addition of optically thin interstellar matter around the model

nuclear AGN region and the ISM is optically thin in all directions ($\tau_V = 0.5$). Our new polarimetric images are shown in Fig. 2

A striking difference between the ISM-free (Fig. 1) and the ISM-included (Fig. 2) polarimetric maps is the shape of the outflowing winds seen in transmission through the dust. The perfect hourglass shape observed when the AGN was in vacuum is now disturbed. The global morphology is more similar to a cylinder, with no flux gradient observed as the photons propagate from the central engine to the far edges of the winds. The overall flux distribution is more uniform throughout the winds, which seems to be in better agreement with what has been observed in the same band, at least for sub-arcsec scales (Packham et al. 1997). At better angular resolutions, polarized flux images are still needed. The polarization position angle has retained its centro-symmetric pattern but the polarization angle is more chaotic at the location of the torus, due to additional dust-scattering. The degree of polarization at the center of the AGN is the same as previously but the integrated map shows a slightly smaller polarization degree (58 %) due to depolarization by multiple scattering.

3 Discussion

Running our radiative transfer codes at 1 μm, we found that a NGC 1068-like model produces the centro-symmetric polarization angle pattern already observed in the optical and infrared bands. Disregarding additional dilution by other sources, the polarization position angle pinpoints the source of emission. Including the ISM in the model does not change the results but tends to decrease the final polarization degree. It also changes the flux repartition in the outflowing winds that act like astrophysical mirrors, scattering radiation from the hidden nucleus. Compared to what has been shown in Gratadour et al. (2015) in the H (1.6 μm) and K (2.2 μm) bands, we find very similar levels of linear polarization at the center of the model, where the central engine is heavily obscured by dust. However, we do not retrieve the distinctive polarization position angle of the torus found by the authors. According to our models, the pattern is at best centro-symmetric rather than directed perpendicular to the outflowing wind axis.

Additional work is needed to explore how such a distinctive pattern can arise at the location of the torus. In particular, adopting the most up-to-date morphological and composition constraints from literature is mandatory to built a coherent NGC 1068 model. Including effects such as polarization by absorption (dichroism) will be necessary. Comparing our results with past linear and circular polarization measurements (e.g, Nikulin et al. 1971; Gehrels 1972; Angel et al. 1976) will drive our models towards the right direction. Finally, the broadband coverage of the codes, from the X-rays to the far infrared, will allow us to robustly test our final model against spectroscopic and polarimetric observations in many wavebands.

The authors would like to acknowledge financial support from the Programme National Hautes Energies (PNHE).

References

Angel, J. R. P., Stockman, H. S., Woolf, N. J., Beaver, E. A., & Martin, P. G. 1976, ApJ, 206, L5
Antonucci, R. 1993, ARA&A, 31, 473
Antonucci, R. R. J. & Miller, J. S. 1985, ApJ, 297, 621
Capetti, A., Macchetto, F., Axon, D. J., Sparks, W. B., & Boksenberg, A. 1995, ApJ, 452, L87
Gehrels, T. 1972, ApJ, 173, L23
Goosmann, R. W. & Matt, G. 2011, MNRAS, 415, 3119
Gratadour, D., Rouan, D., Grosset, L., Boccaletti, A., & Clénet, Y. 2015, A&A, 581, L8
Jaffe, W., Meisenheimer, K., Röttgering, H. J. A., et al. 2004, Nature, 429, 47
Kishimoto, M., Hönig, S. F., Antonucci, R., et al. 2011, A&A, 527, A121
Kishimoto, M., Hönig, S. F., Antonucci, R., et al. 2009, A&A, 507, L57
Kishimoto, M., Hönig, S. F., Beckert, T., & Weigelt, G. 2007, A&A, 476, 713
Lumsden, S., Bland-Hawthorn, J., Moore, T., et al. 1997, Ap&SS, 248, 287
Marin, F., Goosmann, R. W., Gaskell, C. M., Porquet, D., & Dovčiak, M. 2012, A&A, 548, A121
Nikulin, N. S., Kuvshinov, V. M., & Severny, A. B. 1971, ApJ, 170, L53
Packham, C., Young, S., Hough, J. H., Axon, D. J., & Bailey, J. A. 1997, MNRAS, 288, 375
Rowan-Robinson, M. 1977, ApJ, 213, 635
Wittkowski, M., Kervella, P., Arsenault, R., et al. 2004, A&A, 418, L39